British Journal of Healthcare and Medical Research - Vol. 12, No. 05
Publication Date: November 04, 2025
DOI:10.14738/bjhr.1205.19549.
Mayevsky, A. (2025). Cerebral Cortex Physiological Mapping in Health and Disease: From Animal Models to Clinical Applications. *British Journal of Healthcare and Medical Research, Vol - 12(05).* 159-188.

Cerebral Cortex Physiological Mapping in Health and Disease: From Animal Models to Clinical Applications

Avraham Mayevsky
The Mina & Everard Goodman Faculty of Life Sciences and
the Leslie and Susan Gonda Multidisciplinary Brain Research Center,
Bar-Ilan University, Ramat-Gan 5290002, Israel

ABSTRACT

Normal brain cortical activity is an integration of many biochemical and physiological processes including hemodynamic, metabolic, ionic homeostasis and electrical activities. In order to evaluate the functional state of the brain, it is necessary to monitor in real time as many parameters as possible. We developed the concept of "Cerebral Cortex Physiological Mapping" that describes the interrelations between the various parameters measured by the multiparametric monitoring system (MPA). We used these systems in experimental animal models as well as in neurosurgical patients. Our approach aims are to monitor, in real-time, a small volume of the cerebral cortex containing all the tissue elements that are parts of a typical functioning brain tissue. We are interested in the microenvironment of the brain containing neurons, glia, synapses and the microcirculatory elements (small arterioles and capillaries). The various parameters and the technology developed are presented in the attached figure. During the development process we pursued the goal of being minimally invasive in terms of the penetration to the cortical tissue itself. It was obvious that the various probes could not monitor the same volume of tissue due to the size of each probe used. Therefore, we attempted to minimize the diameter of the various probes located in the MPA that had a 5-6 mm contact area with the cerebral cortex. In most of the perturbations used, such as global ischemia, anoxia, hypoxia or hemorrhage, most of the areas in the cortex will respond in the same way. We used these monitoring system in experimental animal models exposed to pathophysiological conditions. Changes in oxygen supply were induced by hypoxia, ischemia or hypeoxia. The level of brain activity was changed by epilepsy or cortical spreading depression. The key monitored parameter, in all monitoring systems, was the oxidation-reduction state of NADH, representing the mitochondrial function in vivo and in real-time. This parameter provided information on oxygen supply as well as oxygen balance in the brain. In the current review, the various systems developed since 1972 will be presented including a typical record of the results obtained.

Keywords: Brain metabolism, NADH Redox State, Tissue energy balance, NADH Fluorescence, *In Vivo* monitoring of mitochondrial NADH.

HISTORICAL OVERVIEW - THE 60 YEAR LEGACY OF PROF. BRITTON CHANCE

My first meeting with Prof. Britton Chance was in Israel during his attendance at the Biophysical Society Meeting in 1971. He came to visit my advisor for my PhD thesis, Prof David Samuel at the Isotope Department of the Weizmann Institute of Science, Israel. He

saw the brain *in vivo* monitoring system for the evaluation of radioactive phosphate, that I developed, and immediately offered me a position in his group as a postdoctoral fellow at the Johnson Research Foundation, the University of Penn, Philadelphia.

After my graduation at the Weizmann Institute (Rehovot, Israel) in October 1972, I moved together with my family (wife and three children) to Philadelphia and stayed there for 2 years. I met Prof. Chance every day in his office/lab, as shown in Figure 1(a). After 2 years of post-doctoral activity, I went back to Bar Ilan University in Israel, but our collaboration continued, and my next visit was for a year from 1980 to 1981. Every year between 1974 and 1988, I visited the Johnson Research Foundation for an average period of 1 month.

Later, we spent 2 years in Philadelphia during which our first attempt to monitor Neurosurgical patients came through. During my collaboration with Prof. Chance, we published 33 papers together, in addition to more than 100 papers that I published with other collaborators on nicotine-amide adenine dinucleotide (NADH) monitoring. Our meeting in 2007 to 2008 in China, as shown in Figure 1(b), was sort of closing a life cycle, which started in Philadelphia in 1972 and ended in the famous Britton Chance Center for Biomedical Photonics, Wuhan National Laboratory for Optoelectronics (WNLO), Huazhong University of Science and Technology (HUST), Wuhan, China.

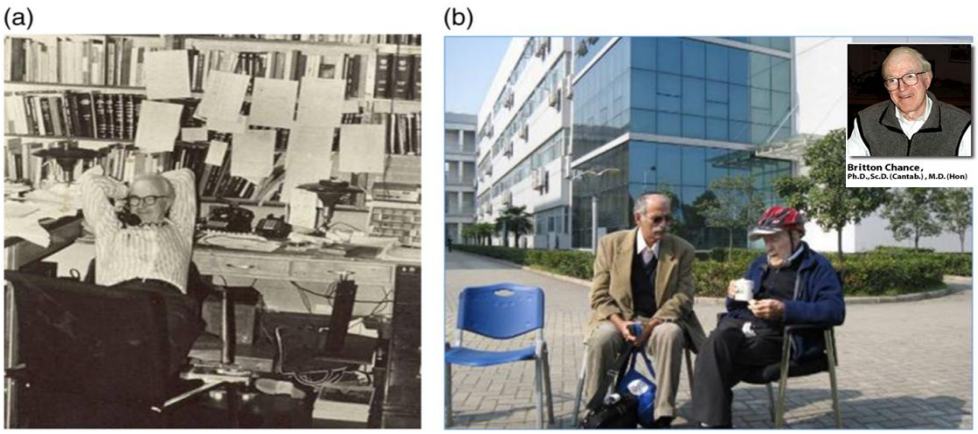

Figure 1: (a) Prof. Chance in his office at the University of Pennsylvania, Philadelphia (1973). (b) My (A. Mayevsky) meeting with Prof. Chance in Wuhan, China (2008).

I would like to summarize his contribution to the field of bioenergetics by monitoring mitochondrial signals using light (Fig. 2). He was the first to develop in detail an optical technique for the monitoring of mitochondrial signals, namely, NADH and Flavoproteins, in intact tissues and later on under *in vivo* conditions.

Prof. Chance started his activities in this field after the discoveries of Warburg and Keilin before 1950. He was the leader of modern biophotonics regarding the theoretical, experimental, and clinical application of optical monitoring of mitochondrial signals. During the first decade (1951 to 1962), he investigated the isolated mitochondria via tissues *in vitro* and finally under *in vivo* conditions. It is impossible to imagine the development of this field of bioenergetics without the foundations put together by Prof. Chance. In the 1970's, he started to apply optical technology to clinical applications.

The Book of Genesis (Bible-Old Testament)

Chapter 1,3

"And God said, Let there be light: and there was light."

Chapter 1,4

"And God saw the light, that it was good: and God divided the light from the darkness."

Figure 2: Citation from the old bible regarding the creation of light.

I would like to mention a few events and episodes that represent my unique personal ties with Prof. Chance (Fig. 1) who was my 'second father' (scientific).

1. Prof. Chance was a very demanding scientist from himself as well as from his collaborators. One day when I was looking for the nitrogen cylinder at 7pm during my experiments, Brit went with the cart to his lab and brought it to my lab. This kind of behavior stimulates our activities and fruitful collaboration. One day, he said "I am waiting for your results for more than 10 years and I am pleased that you are running your studies intensively".
2. My family remembers very well the Sunday sailing event with Brit and others. My children never forgot it.
3. After starting the routine experiments, we had a very stimulating meeting almost every evening. During this short session Brit analyzed the results of the day and we decided about the next day study. Those discussions were recorded and the next day I received the transcript of the discussion.
4. In parallel to his demands, Brit took care of my scientific advancements and provided all my needs in the laboratory and 3 months after my beginning he took me to a meeting (head injury) in the NIH to present my preliminary results. Our first paper was published in mid-1973 after the ISOTT meeting in South Carolina.
5. During my visit in 1980 I collaborated with Dr. Shoko Nioka and Prof. Chance, in applying 31P-NMR to newborn puppies. Most of our studies were run during the night and I remember especially one midnight experiment. Brit went home close to midnight but around 3 a.m. the telephone rang and Brit was asking about the progress of the experiment.
6. Since day one of my collaboration with Brit, he emphasized the needs for translation of the developed technology into a clinical protocols and usage. This approach affected my efforts in this respect and a few papers were published on clinical monitoring of patients during neurosurgical procedures as well as in critical care medicine. I think that Brit's dream came true.

URL: http://dx.doi.org/10.14738/bjhr.1205.19549.

It is now 70 years since the significant work of Chance & Williams on mitochondrial metabolic state *in vitro* was published (Fig. 3), [1-4]. The discovery of the pyridine nucleotides was made by Harden & Young almost 110 years ago [5,6] and was followed by the description of its full structure by Warburg and collaborators 30 years later [7]. All those historical studies led to the first detailed experiments, by Chance et al. [8] in which NADH (Nicotine amide adenine dinucleotide) fluorescence, which was recognized to be a component of Keilin's respiratory chain, was used as a marker of mitochondrial function of the brain and kidney *in vivo* in the anesthetized animals.

METABOLIC STATES OF MITOCHONDRIA AND THE ASSOCIATED OXIDATION-REDUCTION LEVELS OF THE RESPIRATORY ENZYMES

	Characteristics					Steady-state percentage reduction of components				
State	[O_2]	ADP level	Substrate level	Respiration rate	Rate-limiting substance	a	c	b	Flavo-protein*	DPNH
1	>0	low	low	slow	ADP	0	7	17	21	~90
2	>0	high	~0	slow	substrate	0	0	0	0	0
3	>0	high	high	fast	respiratory chain	<4	6	16	20	53
4	>0	low	high	slow	ADP	0	14	35	40	>90
5	0	high	high	0	oxygen	100	100	100	150	100

* These values are based upon the amount of flavoprotein that is reduced upon addition of antimycin A to the mitochondria in state 2 which is ²/₃ the state 5 value.

Figure 3: The definition of mitochondrial metabolic state, *in vitro*, in 1955, by Chance and Williams, opened up a new era in spectroscopic measurements of respiratory chain enzyme's redox state *in vitro* as well as *in vivo* [25].

The discovery of the optical properties of reduced Nicotineamide Adenine Dinucleotide – NADH (earlier names: DPNH - diphosphopyridine nucleotide, or PN - pyridine nucleotide), has led to a very intensive research since the early 1950's. The reduced form of this molecule, NADH, shown in Figure 4A and 4B [9], absorbs light at 320-380 nm (Fig.4C) and emits fluorescent light at 420-480 nm range (Fig. 4D) [10]. As the oxidized form NAD^+ does not absorb light in this range, it was possible to evaluate the redox state of the mitochondria by monitoring the UV absorbance or Blue fluorescence of NADH.

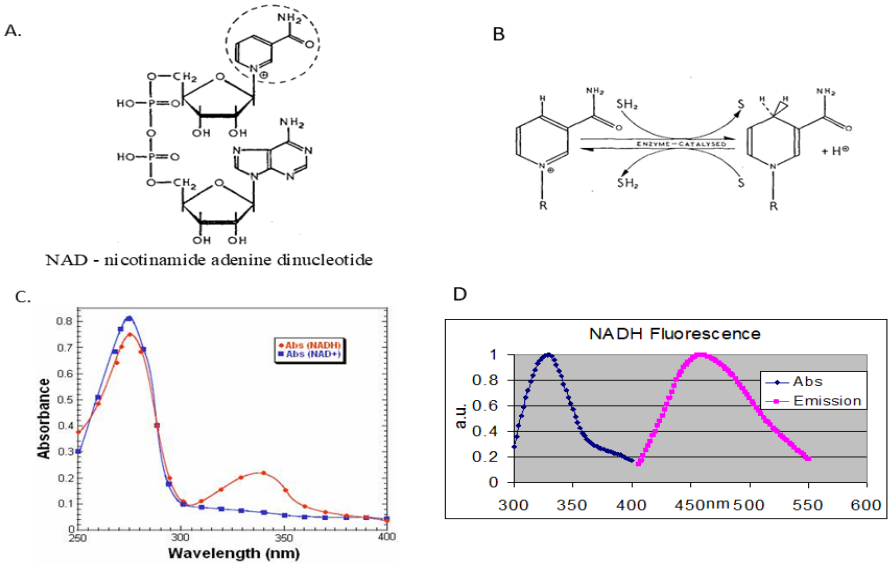

Figure 4: A. The structures of NAD^+ The nicotinamide group (broken ring) is the "functional" part of both molecules i.e. the portion of the molecules where oxidation and reduction take

place [9,90]. B. The transition between oxidized and reduced NADH. C. Absorption Spectra of NAD^+ and NADH. D. Excitation and emission spectra of NADH [10].

In 1951, Theorell and Bonnichsen found a shift in the absorption spectrum of DPNH upon addition of alcohol dehydrogenase (ADH) [11]. In the same year, Theorell and Chance described a new spectrophotometric technique for measuring the formation and disappearance of the compound of ADH and DPNH [12]. This work was based on previous publications that also appeared in 1951 [13]. Moreover, in 1951, Chance & Legallias described a rapid and sensitive spectrophotometer for the measurement of reaction kinetics [14]. A year later (1952), Chance and Castor showed the applicability of this new technique to the measurements of pyridine nucleotide enzymes of muscle homogenate or intact cells [15]. In this study they casted the doubt about Warburg's assumption that the Warburg effect was due to suppressed mitochondrial function. Immediately afterwards (1952), Chance used the same device to monitor respiratory pigments, including NADH, in metabolizing cells [16]. Chance and Neilands (1952) found that the interaction between NADH and Lactic Dehydrogenase (LDH) of the heart led to a shift in the absorption band [17]. In 1952 and 1953, Chance and Castor showed the dynamics of respiratory pigments behavior (including NADH) in Ascites tumor cells [18]. In 1954, Chance and Williams briefly described new sensitive differential spectrophotometric methods applied to the study of reduced NADH in isolated rat liver mitochondria [19]. The same approach was used by Connelly and Chance in monitoring NADH in stimulated frog nerve and muscle preparations [20]. The oxidation of NADH in the muscle was similar to its oxidation in isolated mitochondria upon addition of ADP. In a comprehensive paper on "Enzyme mechanisms in living cells" Chance described in detail the measurements of the respiratory enzymes, including NADH [21].

A major milestone in NADH monitoring was the technique presented in 1954 by Chance [22] using a double beam spectrophotometer to determine the appropriate wavelengths in measurements of respiratory enzymes. The detailed descriptions of the respiratory chain and oxidative phosphorylation in the mitochondria – published in 1955 by Chance & Williams – established our basic knowledge of the mitochondrial function [1-3,23,24]. In the latter five papers, Chance and Williams defined, for the first time, the metabolic states of isolated mitochondria *in vitro*, depending on the substrate, oxygen and ADP levels (Fig. 3). In addition, they correlated those metabolic states to the oxidation-reduction levels of the respiratory enzymes. The physiological significance of those metabolic states was discussed in 1956 by Chance & Williams [25], and later by Chance and other collaborators [26-30]. In 1959, Chance et al. described a highly sensitive recording microspectrophotometer that enabled the monitoring of NADH absorbance in a single cell [31].

Monitoring of NADH Fluorescence

The fact that NADH was monitored by the difference in the absorption spectrum of its reduced form, limited the use of that technique to the study of mitochondria *in vitro*, and in very thin tissue samples (e.g. muscle) or in cell suspension. To provide a method more specific than absorption spectroscopy, fluorescence spectrophotometry in the near-ultraviolet range (UV-A) was applied for NADH measurement. The initial model of fluorescence recorder was described by Theorell & Nygaard in 1954 as seen in Figure 3.5 [32,33] and Theorell, Nygaard and Bonnichsen [34]. Using a modified device, Boyer & Theorell (1956) showed that the fluorescence of DPNH was shifted and the intensity was increased upon combination of DPNH and liver alcohol dehydrogenase-ADH [35]. The first detailed study using fluorescence spectrophotometry

URL: http://dx.doi.org/10.14738/bjhr.1205.19549.

of NADH in intact Baker's yeast cells and Algae cells, was published in 1957 by Duysens & Amesz [36].

In the next 5 years (1958-1962), the monitoring of NADH fluorescence was significantly expanded, led by Chance and collaborators. In a first preliminary study, Chance et al. [37] performed simultaneous fluorometric and spectrophotometric measurements of the reaction kinetics of bound pyridine nucleotides (PN) in the mitochondria. In the same year (1958) Chance and Baltscheffsky presented preliminary results of measuring the fluorescence of intramitochondrial PN as seen in Figure 3.8B [38]. In this study, they proved the connection between the mitochondrial metabolic state and the redox state of NADH as measured by spectral fluorometry in mitochondria isolated from rat liver [1].

The correlation between the enzymatic assay of PN and sensitive spectrophotometry was investigated by Klingeberger et al. using rat liver, heart, kidney and brain [39]. In 1959 Chance and collaborators were able to expand the use of NADH fluorometry to various experimental models, from isolated mitochondria to intact tissue. Intramitochondrial pyridine nucleotides were analyzed in connection to the ADP-ATP cycle [40]. In order to monitor NADH localization in intact cells, Chance and Legallais developed a unique differential microfluorimeter with a very high spatial resolution [41]. This approach was used, in various cells, to identify the intracellular localization of NADH fluorescence signals [42-44]. The next step was to apply the fluorometric technique to the higher organization level of animal tissues. Together with Jobsis, Chance measured *in vitro* changes in muscle NADH fluorescence following stimulation [45]. In another paper published by Chance and Theorell [46] the authors came to the very significant conclusion that "The oxidation and reduction state of mitochondrial pyridine nucleotide without a measurable change of cytoplasmic fluorescence suggest that compartmentalization of mitochondrial and cytoplasmic pyridine nucleotide occurs *in vivo*, at least in the grasshopper spermatid." In another paper, Chance and Hollunger elaborated on the energy-linked reduction of the mitochondrial pyridine nucleotides [47].

An intensive use of the *in vivo* NADH monitoring approach started in 1962. The "classical" paper on *in vivo* monitoring of NADH was published in 1962 by Chance et al. [8]. They were able to simultaneously monitor the brain and kidney of anesthetized rats using two microfluorometers. In 1962, Chance and collaborators elaborated on this kind of *in vivo* monitoring and used it in other rat organs [48-50].

In 1959, Chance & Legallais [41] described a differential fluorometer that heralded a new era in monitoring NADH fluorescence *in vivo* as an indicator of mitochondrial function. They used a microscope, serving as the fluorometer basis, with two light sources: tungsten and mercury lamps with appropriate filters. In 1959, Chance & Jobsis [45] and Chance [29] proved that mechanical muscle activity is associated with NADH oxidation measured in excised muscle. This study was the bridge from the subcellular (mitochondria) and cellular (intact cell) monitoring approaches toward actual *in vivo* applications.

The first *in vivo* NADH monitoring device was presented in the late 1950's and early 1960's. At that stage, the effects of scattered light and tissue absorption due to blood were not taken into consideration when monitoring NADH fluorescence. The first detailed results of *in vivo* NADH fluorescence measurements were published in 1962 [8].

These "classical" papers described two microfluorometers that were modifications of previous designs [41,43]. This micro-fluorometer (Fig. 5A) type employed Leitz "Ultrapack" illumination, which had been used for many years by various groups until the appearance of UV transmitting optical fibers. In order to avoid movement artifacts, rats were deeply anesthetized and their heads were fixated in a special holder attached to the operation table. Numerous studies utilized the principles of the "Ultrapack" illumination system. The same instrumentation was used in other *in vivo* studies, including those of Chance's group [50-55].

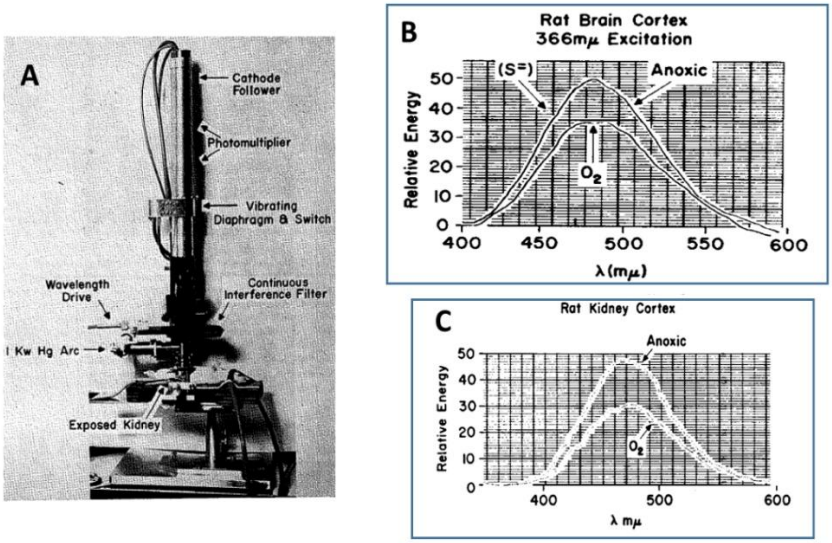

Figure 5: A. Microspectrofluorometer developed by Chance et al that was used in the 1960's. In addition to the interference filter, a Wratten type 2C filter is also placed in the back aperture of the objective. The wave-length-range of the interference filter is 400-700 mμ, and the specification on its spectra interval is 30-40 mμ. Other features of the high pressure mercury arc excite the fluorescence of the specimen at 366 mμ by means of an 'Eppendorf' primary filter. Fluorescence excitation and emission pass through the Leitz Ultrapak objective (×11) and a ×3 ocular [50]. 5B and 5C - The emission spectra of rat kidney (C) and rat brain cortex (B), under aerobic conditions (lower trace) and under anoxic conditions (upper trace) [56].

The use of NADH fluorometry for *in vivo* studies started at the end of the 1950s and has been presented in various publications. In a summative study, Chance compared spectra of NADH measured from rat kidney cortex to those of rat brain cortex (Figs. 5B and 5C) and found that the main effect of anoxic transition, both in the kidney and the brain, was a large increase in the fluorescence intensity with no detectable shift in the spectra [56].

As described by Chance and Williams [1,25] the complete depletion of O_2 from the mitochondria inhibits oxidative phosphorylation and terminates ATP production. This situation destroys the normal function of the tissue, and cell death can ensue. In this book, we define anoxia as a complete deprivation of O_2 caused by breathing 100% N_2. Hypoxia implies that the deprivation of O_2 from the breathing mixture is partial and ranges between 21% (normal air) and 0% (anoxia). Ischemia is defined as a decrease in O_2 supply due to a decrease in blood flow to the monitored organ. The degree of ischemia can vary from a full absence of flow (complete ischemia) to various levels of blood flow (partial ischemia). Although oxygen deficiency is the main event in each of the three experimental conditions (anoxia, hypoxia and ischemia), other physiological factors may differ. For example, microcirculatory blood flow is decreased under

URL: http://dx.doi.org/10.14738/bjhr.1205.19549.

ischemia, but increases under brain hypoxia. Thus, changes in the tissue due to other blood flow related factors are not identical.

The responses to hypoxia and anoxia are very similar; therefore, they will be discussed together. According to the definition of Chance & Williams [1,4], a shift toward State 5 involves an increase in NADH proportional to a decrease in O_2 supply. Figure 6 demonstrates the response of the brain to hypoxia (A) and anoxia (B) published by Chance in the early days of NADH monitoring *in vivo* [49,57]. At those days the fluorescence was measured and displayed without correction for hemodynamic artifacts which was developed later in time. A clear increase in NADH fluorescence was recorded under the deprivation of oxygen. Similar responses of the brain and the kidney to anoxia were recorded in part B.

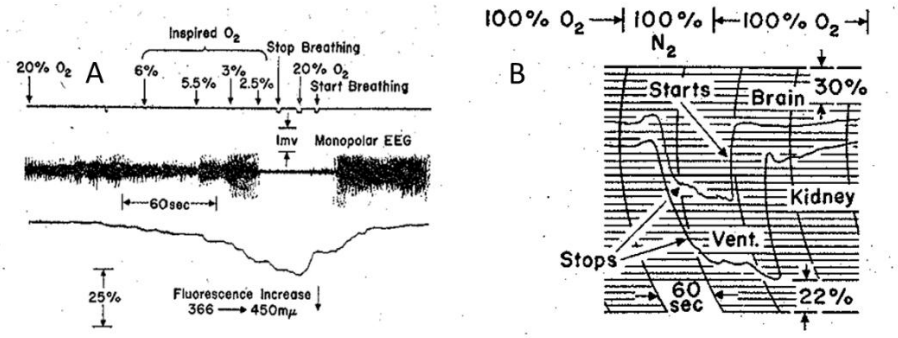

Figure 6: A. Correlation between EEG and pyridine nucleotide reduction in the slow transition from aerobiosis to anoxia. The top trace includes the measurements of inspired oxygen concentration according to the Pauling oximeter [49]. B. Simultaneous recordings of fluorescence changes in rat brain and rat kidney in a cycle of anoxia. Fluorescence increases are indicated in a downward direction [57].

The first time that NADH was monitored *in vivo* in more than 1 site simultaneously was reported by Chance et al in 1962 [8]. They used two units of the same type of fluorometer placed on two organs in the same rat. Two organs were exposed in the same rat, namely the brain and the kidney. In this study they exposed the animal to various perturbations including anoxia and adrenaline injection. Figure 7A shows the probes located above the brain (right side) and the kidney (left side). Typical response of the kidney (part 7B left side) to anoxia and the brain to hypoxia (part 7B right side) are presented. The results were presented on two recorders. Therefore, the quantitative comparison between the responses was not possible.

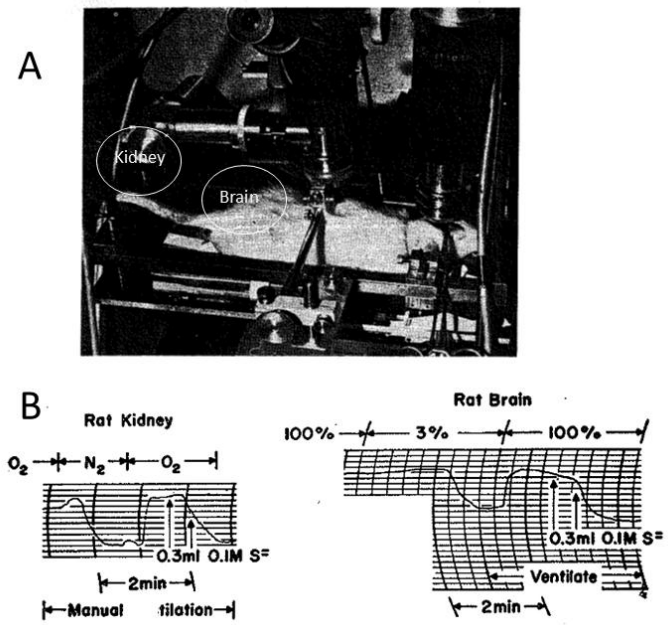

Figure 7: A. Experimental arrangement for simultaneous microfluorometry of brain and kidney cortex in the rat. Two microfluorometers are focused on the exposed surfaces of the brain and kidney. By means of a tracheal cannula the oxidation-reduction level of the intracellular pyridine nucleotide can be altered and the corresponding fluorescence changes can be recorded by the two microfluorometers. B. Micro-fluorometric recording of fluorescence increases caused by oxygen-nitrogen transition and by sulfide infusion into the vena cava, for kidney (*left*) and brain cortex (*right*) of a urethane-anesthetized rat. The inspired gas was changed from oxygen to nitrogen for the kidney, and from oxygen concentrations of 100 percent to concentrations of 3 percent for the brain. The time scale proceeds from left to right, and increase in fluorescence is indicated as a downward deflection. In both experiments the oxygen-nitrogen-oxygen transition is followed by slow infusion of a solution of 0.1 M sulfide. The records indicate that the increase in fluorescence caused by sulfide inhibition of cytochrome oxidase is about the same as, or greater than, that observed in the oxygen-nitrogen transition, where hemoglobin is deoxygenated as well. The sensitivity in recordings on the brain is 2.5 times that in recordings on the kidney [8].

BRAIN AND TISSUE ENERGY METABOLISM AND MITOCHONDRIAL FUNCTION

The functional capacity of any tissue is related to its ability to perform its work. It is possible to assess this ability through the knowledge of changes in the oxygen balance, i.e. the ratio of oxygen supply to oxygen demand in the tissue. Schematic presentation of the balance between oxygen supply and demand in a typical tissue is shown in Figure 8. The supply of oxygen is dependent upon microcirculatory blood flow and the level of oxygen bound to the hemoglobin in the small blood vessels. The saturation of hemoglobin is affected by the oxygen gradient between room air through the large arteries, and small arterioles to the intracellular space and finally the mitochondrion. The demand for energy is affected by the specific activities taking place in each organ. The intracellular level of mitochondrial NADH (the reduced form) is a parameter related to the energy balance.

URL: http://dx.doi.org/10.14738/bjhr.1205.19549.

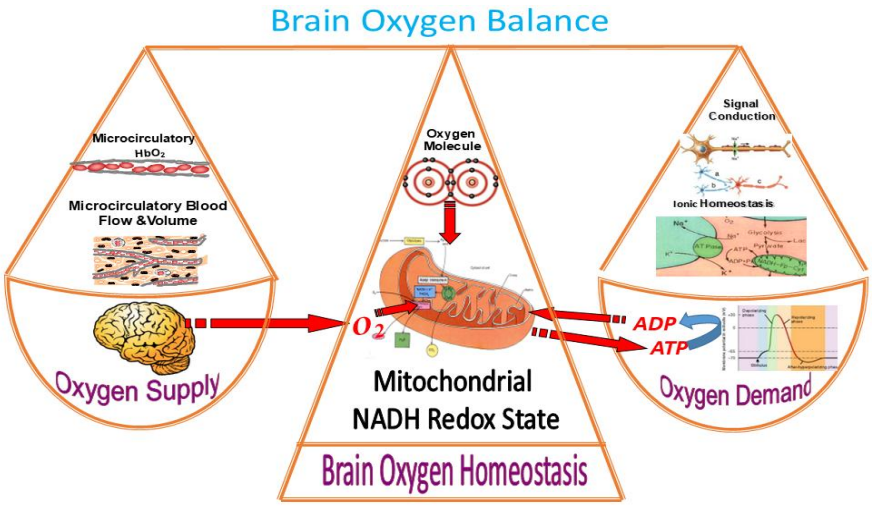

Figure 8: Presentation of Brain Oxygen Balance or Brain Oxygen Homeostasis evaluated by the ratio between brain oxygen supply and brain oxygen demand [91]. Energy supply is measured by tissue blood flow (TBF), hemoglobin Oxygenation and partial pressure of Oxygen which is similar in all tissues. Energy demand is affected by Ionic Homeostasis, and Signal Conduction. Mitochondrial NADH redox state serve as an indicator for brain energy or oxygen balance [92].

Figure 9 presents the involvement of the mitochondria in cellular energy metabolism. Substrates and O_2 are supplied and regulated by the blood in the microcirculation, namely from the very small arterioles and the capillary bed. The main function of the mitochondria is to convert the potential energy stored in various substrates (e.g. Glucose) into ATP. The inner membrane of the mitochondria contains 5 complexes of integral membrane proteins, including NADH dehydrogenase (Complex 1). Three of those proteins are involved in the respiratory chain activity. The main function of the respiratory chain is to gradually transfer electrons from NADH and $FADH_2$ (originating from the Krebs cycle) to oxygen (O_2). With the addition of protons (H^+), water molecules (H_2O) are generated in Complex 4. NADH is a substrate or a coenzyme for the enzymatic activity of dehydrogenases that form part of the respiratory chain and reside in the inner membrane of the mitochondria. Further details on the biochemical properties of NADH can be found in publications by Chance and his collaborator [43,46]. The formation of ATP depends on the sufficiency of substrate (i.e. glucose) and oxygen supply to the tissue by the blood flow in the microcirculation (Fig. 9). Without the sufficient supply, cells cannot function properly and can, ultimately, die. Since most of the energy consumed by tissues is dependent upon the availability of oxygen, the terms “energy” and “oxygen” will be used here synonymously.

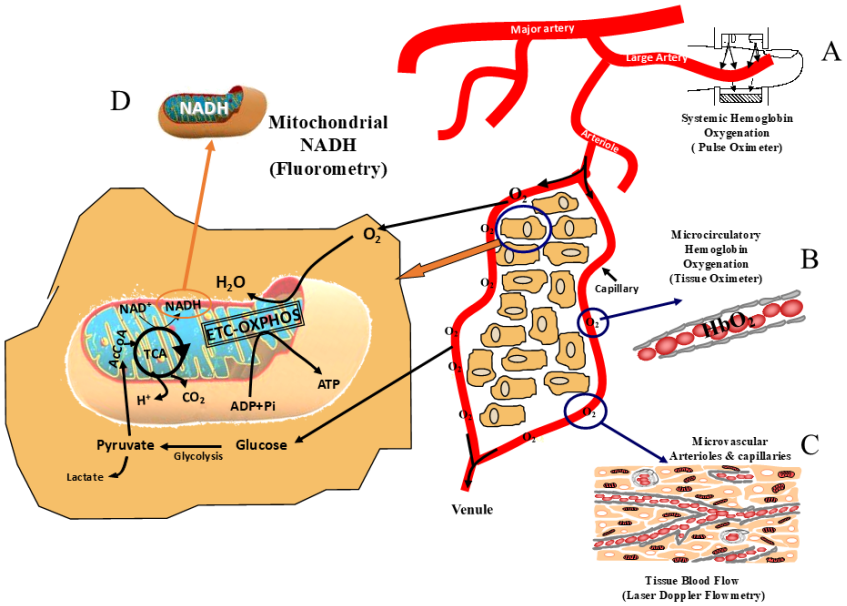

Figure 9: The available techniques for real time monitoring of energy metabolism at the tissue level. Part A shows the coupling between the macro-circulation monitored by the Pulse oximeter and the microcirculation. B-D monitoring of vascular and intracellular compartments (see text for details) [10].

The electron transfers (oxidations/reductions) down the respiratory chain result in the production of adenosine tri-phosphate (ATP). Concomitantly with the electron transport, the respiratory chain components switch between reduced and oxidized states, each of which has different spectroscopic properties. Hydrolysis of the pyrophosphate bonds provides the energy necessary for the cell's work. In order to assess the energy demand, it is necessary to measure different organ-specific parameters. For example, in the brain, the energy demand can be evaluated by measuring the extracellular levels of K^+ that reflect the activity of the major ATP consumer Na^+/K^+-ATPase [58,59]. In the heart, most of the energy is consumed by muscle contraction activity. On the other hand, the energy supply mechanism is the same for all tissues: oxygenated blood reaching the capillary bed releases O_2 that diffuses into the cells. Therefore, it is possible to evaluate tissue energy supply by monitoring the same four different parameters in all tissues. Energy exchange depends on pO_2 (partial oxygen pressure) in the tissue. Information regarding pO_2 in the tissue, therefore, is helpful for the evaluation of tissue metabolic activity. Oxygen levels can be measured by oxygen electrode however the sensitivity and accuracy of oxygen electrodes in the range of 1 mmHg (intracellular level) is not sufficient for the evaluation of mitochondrial function. The need for an intracellular pO_2 indicator, as a physiological and biochemical parameter of living tissue, has emerged more than 60 years ago. Mitochondria are the intracellular organelles that consume most of the oxygen. Therefore, the redox state of electron carriers in isolated mitochondria *in vitro* as well as *in vivo* as a function of oxygen concentration has been extensively studied. Chance et al concluded that "For a system at equilibrium, NADH is at the extreme low potential end of the chain, and this may be the oxygen indicator of choice in mitochondria and tissue as well" [60]. Lubbers in 1995 concluded that "the most important intrinsic luminescence indicator is NADH, an enzyme of which the reaction is connected with tissue respiration and energy metabolism" [61]. As of today, the ability to measure tissue energy metabolism at the microcirculation and cellular level is relatively limited.

URL: http://dx.doi.org/10.14738/bjhr.1205.19549.

REAL TIME MONITORING OF TISSUE VITALITY

Several real-time invasive and noninvasive techniques have been developed to determine tissue energy metabolism or tissue vitality *in vivo*. A short description of the available techniques for monitoring tissue energy balance described by various investigators is presented in Figure 9. These techniques could be adapting and used in experimental animals as well as in patients. In order to present the linkage between the systemic and the tissue level oxygenation, the pulse oximeter technique is shown in the same Figure 9, although the signal is not originated from the microcirculation.

Systemic Pulse Oximetry (A)

This standard of care device is measuring the oxygenation level of the hemoglobin dependent on the pulse passing in the large arteries. Therefore, this technique can't provide information on hemoglobin saturation in the microcirculation.

Microcirculatory Hb Oxygenation (B)

Oxygenated hemoglobin can be monitored at the microcirculatory level using the absorption spectrum of hemoglobin**,** which is different in its oxygenated or deoxygenated state. One possibility is to illuminate the tissue with 585 nm light which is an isosbestic point, and with 577 nm light, which is a non-isosbestic point, in which the oxy-hemoglobin absorb more light than the deoxy-hemoglobin form. By subtracting the 585 nm reflectance from the 577 nm reflectance, a parameter correlated to blood oxygenation is obtained. A detector collects the light reflected from the tissue and converts it into oxy-hemoglobin levels [62,63].

Microcirculatory Blood Flow (C)

Real time monitoring of tissue blood flow (TBF) can be achieved using laser Doppler flowmetry (LDF) [64-66]. The LDF measures relative changes, which correlate with the relative TBF alterations. The principle of LDF is to measure the Doppler shift, namely, the frequency change undergone by the light reflected from moving red blood cells. The results are presented as percentages of a full scale (0%-100%), providing relative perfusion values. In our laboratory, we used LDF to measure TBF (tissue blood flow) in the brain, kidney, and liver [67-69]. This method has been successfully employed in many animal models, including rodents, cats and baboons under stroke [70].

Mitochondrial NADH (D)

NADH monitoring from the organ surface (brain, kidney, liver, testis, etc.) is performed by the fluorometric technique based on the original work by Chance and Williams [1,58]. The excitation light (366 nm) is passed from the fluorometer to the tissue through a bundle of quartz optical fibers. The emitted light (450 nm), together with the reflected light at the excitation wavelength, is transferred to the fluorometer through another bundle of fibers. The measured changes in fluorescence and reflectance signals are calculated as percent values relative to the calibrated signals under normoxic conditions. This type of calibration is not absolute, but it provides reliable and reproducible results for different animals and different laboratories [58,59]. The combination of NADH fluorescence and LDF techniques has been routinely utilized in our laboratory for the past 30 years [67,71-73].

CEREBRAL CORTEX PHYSIOLOGICAL MAPPING

Normal brain cortical activity is an integration of many biochemical and physiological processes including hemodynamic, metabolic, ionic homeostasis and electrical activities. In order to evaluate the functional state of the brain, it is necessary to monitor in real time as many parameters as possible. We developed the concept of "Cerebral Cortex Physiological Mapping" that describes the interrelations between the various parameters measured by the multiparametric monitoring system (MPA). We used these systems in experimental animal models as well as in neurosurgical patients. As can be seen in Figure 10, our approach aims to monitor, in real-time, a small volume of the cerebral cortex containing all the tissue elements that are parts of a typical functioning brain. We are interested in the microenvironment of the brain containing neurons, glia, synapses and the microcirculatory elements (small arterioles and capillaries). The various parameters and the technology developed are presented in Figure 10. During the development process we pursued the goal of being minimally invasive in terms of the penetration to the cortical tissue itself. It was obvious that the various probes could not monitor the same volume of tissue due to the size of each probe used. Therefore, we attempted to minimize the diameter of the various probes located in the MPA that had a 5-6 mm contact area with the cerebral cortex. In most of the perturbations used, such as global ischemia, anoxia, hypoxia or hemorrhage, most of the areas in the cortex will respond in the same way.

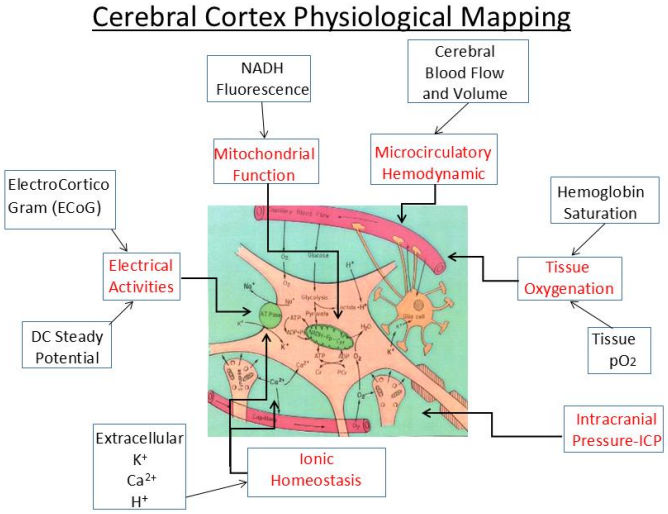

Figure 10: Schematic presentation of the concept "Cerebral Cortex Physiological Mapping" used in our studies to be discussed in the current paper. The available techniques for real time monitoring of Cerebral blood flow, mitochondrial function, ionic homeostasis and electrical activities in the intact brain are presented [92]. (Modified)

Monitoring NADH Fluorescence and Reflectance

In order to enable the monitoring of NADH fluorescence in unanesthetized animals or other *in vivo* preparations, a flexible means was needed to connect the fluorometer with the tested organ, for example the brain. This was achieved in 1972, when UV transmitting quartz fibers became available (Schott Jena Glass, Germany). We have used the light-guide-based fluorometer for *in vivo* monitoring of the brain [60,74] subjected to anoxia or cortical spreading depression. The historical development of light-guide-based fluorometry-reflectometry is shown in Figure 11A-D. The original device functioned on the time sharing principle (Fig. 11A),

URL: http://dx.doi.org/10.14738/bjhr.1205.19549.

where 4 filters were placed in front of a 2 arms light guide. Filters 1 and 3 enabled the measurement of NADH fluorescence, while filters 2 and 4 were used to measure tissue reflectance at the excitation wavelength. The reflectance trace was used to correct the NADH signal for hemodynamic artifacts, and to indicate changes in the blood volume of the sampled tissue.

In this original system, only one photomultiplier tube was used for the detection of the two signals. Figure 11B presents one of the first *in vivo* brain monitoring time sharing setups, the time sharing approach (AC mode) was replaced by splitting the light emitted from the tissue into two unequal fractions for the measurement of fluorescence and reflectance signals. This model, named the DC type fluorometer, had originally a 3-way light guide which was later replaced by a two arms light guide probe (Fig. 11C). In all the three configurations, the reflectance signal was used for the correction of the fluorescence signal. Our group developed and used the model shown in Figure 11C in the late 1970's. This model is still being used in our laboratory to monitor the brain, heart, liver, kidney, as also in multi-site or multi-organ monitoring. The responses to anoxia using different diameter of the fiber optic bundle are shown in Figure 11D.

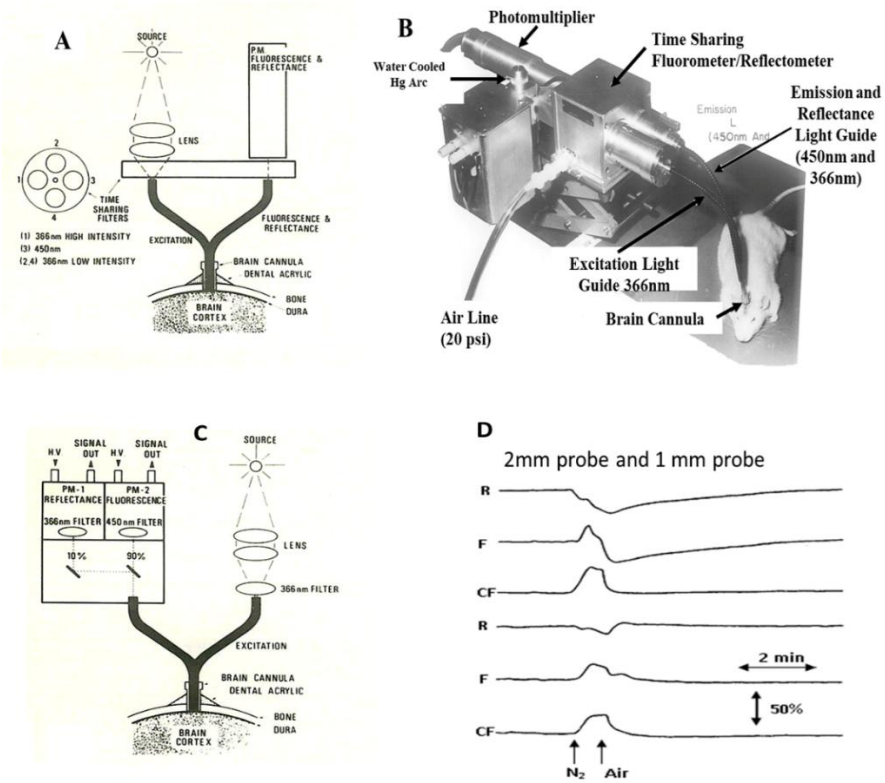

Figure 11: A. Time sharing fluorometer/reflectometer connected to a rat brain cannula by a flexible y shape light guide [58]. B. Picture of the time sharing fluorometer reflectometer used in the 1970th. The rat brain is connected to the device by a flexible fiber optic probe [58]. C. The structure of the standard DC fluorometer/ connected to the brain of a small animal [58]. Excitation (right), Emission (left) - optical fibers for the monitoring of NADH redox state. H.V. - high voltage; PM - photomultiplier. D - The effect of the monitored tissue volume (the diameter of the fiber optic probe) was tested under anoxia as shown in B, upper 3 traces (2 mm diameter) and lower 3 traces (1 mm diameter) [58].

Preparing the Animal for Monitoring

Using of the optical technique for monitoring of NADH fluorescence requires a stable contact between the fiber optic probe and the tissue. Movement artefacts will affect the stability of the monitored signals. In order to achieve this stability, we developed the following 4 techniques that were applied to various organs.

A. Cementation, used in brain studies including unanesthetized small animals.
B. Adhesion, used in monitoring soft tissues and visceral organs.
C. Suturing could be used in monitoring heart or skeletal muscle.
D. Use of micromanipulator in monitoring the spinal cord or other organs.

Surgical Procedures

A special table and probe holding device was constructed in order to perform brain as well as other organs preparation for the monitoring period.

Monitoring the Brain

The brain is operated while the head is connected to a special head holder for the period of the operation (20-30 minutes) and then could be released, for the monitoring period, as shown in Figure 12. The other monitored organs i.e. muscle, kidney or liver have to be held by a micromanipulator during the monitoring period. As mentioned before, the brain was the main organ monitored by other investigators as well as in our group. In order to be acquainted with the NADH monitoring device it is recommended to start with brain monitoring and later on to move and use the selected organ. The reason for it is that the connection between the fiber optic probe and the monitored tissue must be constant during the monitoring session and in the brain it is easy to be achieved by connecting a probe holder to the skull using acrylic cement as shown in Figure 12B.

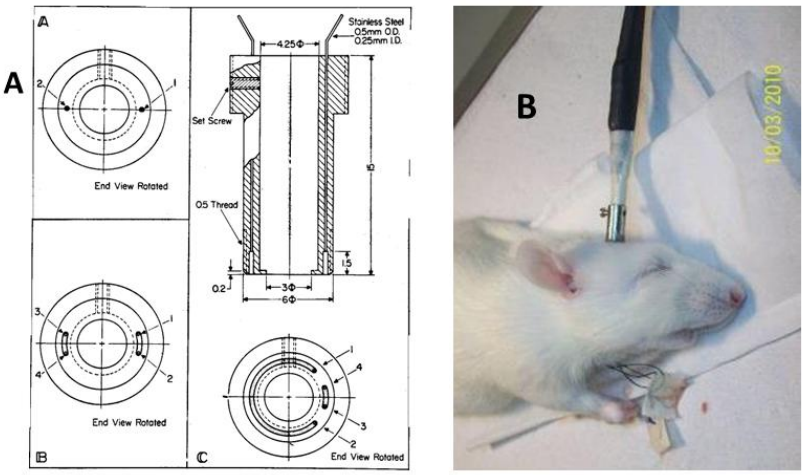

Figure 12: A. The construction of the Light guide holders (cannulas) for measurement of NADH fluorescence from the surface of the brain of an awake rat in experiments in which topical application of drugs is needed. B. After the insertion of the fiber optic probe to its holder the animal is ready for the monitoring [10].

A midline incision is made in the skin, exposing the skull. Three holes were drilled in the skull and appropriate small screws were inserted to the skull (less than 1 mm in depth). An appropriate hole (3-5 mm in diameter) was drilled in the right or left parietal bone for the

URL: http://dx.doi.org/10.14738/bjhr.1205.19549.

fixation of a light guide holder in which the monitoring probe was inserted later on. The light guide holder and the 3 screws were then fixated to the skull using dental acrylic cement. Ten minutes later the head of the animal was released from the head holder and the probe was inserted to a predetermined depth and fixed by a set screw (Fig. 12B).

The structure of the standard DC fluorometer/reflectometer connected to the brain of a small animal were shown. The thread outside the bottom of this cannula enables screwing it into the skull and also gave a better connection between the cannula and the cement. The cannula shown in Figure 12 was used in experiments in which animals were exposed to nitrogen/oxygen breathing cycles or to hyperbaric pressure of oxygen. The EEG was measured between the two electrodes, 1-2, cannula type B was used in all experiments in which spreading depression was elicited by application of KCl solution above the Dura. The KCl electrodes 1,2-3,4. The third type, C, has two compartments in the bottom, the small one for KCl application 3-4 and the large compartment, 1-2, where chemicals such as Metrazol were applied and was affecting larger area. A fifth electrode was located 180° to electrodes 3-4, so the EEG was measured at the same time. We have used a short anoxic episode (20-30 sec) in order to test the intactness of the tissue. If the NADH response to anoxia was too small, we stopped the experiment, because it indicated that the brain was damaged and NADH was already elevated.

Results and Discussion

In this section we will present and discuss the stages of the monitoring system development and data collected by these systems.

Fiber Optic Based Fluorometer and EEG:

During the initial step we developed the fiber-optic-based fluorometer/reflectometer for monitoring of mitochondrial NADH in anesthetized or unanesthetized animal [74]. Various types of fiber optic probes were developed during the years. In order to keep a direct and constant contact between the brain and the probe, special design holders were developed during the years. The first fiber optic probe was described in 1973 [59,75] and the other types were presented in our review paper [76]. After the end of the operation, the probe was inserted into the holder that was cemented to the skull.

Figure 13 shows typical 2 responses obtained in a rat experiment. As can be seen, we monitored 2 signals by the Fluorometer, namely, the NADH fluorescence at 450 nm and the total back scattered light at the excitation wavelength (366 nm) called Reflectance. In addition to NADH we monitored EEG activity by placing two stainless steel electrodes on the brain surface. In Part A, the complete elimination of oxygen led to a large increase in the NADH and the EEG signal disappeared very fast. In this animal the change in the reflectance was very small as compared to most of the rats. As soon as the rat started to breathe air, the NADH level recovered very fast. In part B, the effect of brain activation induced by Cortical Spreading Depression (CSD) is shown. In this response the Blood volume changes concomitantly with the mitochondrial NADH. The NADH redox state was shifted to more oxidized state due to the increase in ATP demand. The CSD developed only in the stimulated hemisphere, as seen in the ECoG, while the contra lateral hemisphere served as a control. The same monitoring system was used in other studies [77].

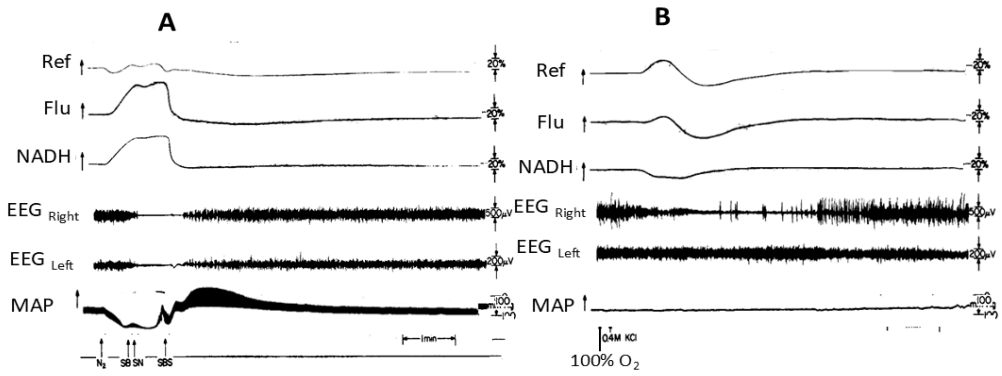

Figure 13: A. Typical response of the rat brain and the systemic blood pressure (MAP) to a nitrogen cycle. Ref - Reflection; Flu – Fluorescence; MAP - mean arterial pressure; SB - stop breathing; SN - stop nitrogen; SBS - start breathing spontaneously. B. The response of the brain to the application of KCl (0.4 M) on the dura surface under hyperoxia (100% O_2) [74].

NADH and pO_2 Measurements:

Since mitochondrial NADH is sensitive to intracellular levels of oxygen we had developed a MPA that contained a surface oxygen electrode in combination with NADH and ECoG (Fig. 14A). It is important to note that oxygen electrode readings are averaging the oxygen level in the vascular, extracellular and intracellular compartments [78].

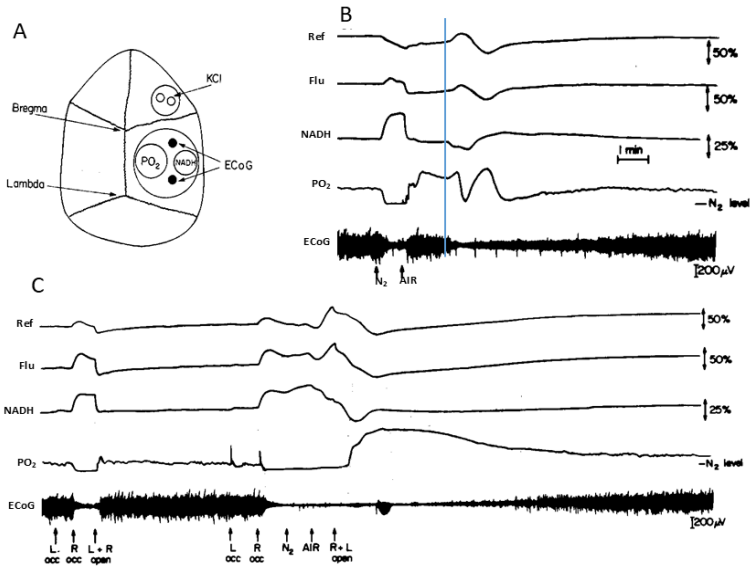

Figure 14: A. Schematic presentation of the various probes location on the surface of the gerbil brain. The large cannula contained the light guide for NADH measurement, the pO_2 and ECoG electrodes. The cannula for KCl application was located 2-3 mm anterior to the large cannula. B. The effects of anoxia and carotid arteries occlusion on the metabolic and electrical activity of the awake (B) and anesthetized (C) gerbil brain [78].

Typical results of this MPA are in Figure 14(B & C). The response to anoxic episode, shown in part B, is typical to the lack of oxygen, namely, a sharp drop in pO_2 and a large increase in NADH. At the recovery phase, the pO_2 response to CSD presented has a unique nature. One minute after

URL: http://dx.doi.org/10.14738/bjhr.1205.19549.

breathing was started, a biphasic response was recorded inversely related to the reflected light changes, namely, that when the reflectance showed an increase, the pO_2 trace showed a parallel decrease; and when the reflectance showed a large decrease (increased blood volume) the pO_2 showed three-to four-fold increase, and then gradually recovered to the normoxic level in parallel to the gradual increase in the reflected light.

The biphasic response in the pO_2 trace is in correlation to the response of the NADH fluorescence trace and we assume that it is the typical response to CSD, as described previously [79] after anoxic cycle.

Figure 14C presents the effects of unilateral or bilateral carotid artery occlusion. In this animal the occlusion of the contralateral carotid artery (Locc) had a very small effect on the NADH or the pO_2. Occlusion of the right carotid (while the left one was closed) induced a large fall in pO_2 and an increase in NADH with similar kinetics. The recovery after bilateral recirculation was fast, without any significant overshoot in the pO_2. In the second ischemia episode, when nitrogen was applied to the ischemic brain, a large overshoot in the pO_2 was recorded after recirculation. The large increase in pO_2 was parallel to the large decrease in reflectance with the same kinetics toward the normoxic level. The NADH shows an oxidation cycle after recirculation due to CSD, as can be seen in the ECoG trace.

The First Multiparametric Monitoring System:

Our aim was to provide a new holding system allowing an easy implantation of surface probes in various combinations on the brain of small mammals and to reevaluate the potential of such surface electrode assemblies in tracing physiological and pathological events [80]. In this stage we added to the basic assembly system the measurements of extracellular tissue pH and K^+, DC potential and local temperature, in addition to the other parameters, including NADH fluorescence, reflected light and electrocorticogram (ECoG). Ideally, the multiprobe assembly designed (Fig. 15) for our project had to be rugged enough to withstand routine use by non-specialists and yet be miniaturized enough to fit the limited surface available for implantation on rat and gerbil skulls (about 6-7 mm in diameter on each hemisphere). For ischemic studies, our interest was focused on monitoring mean values over large areas, suggesting the use of larger electrodes. In contrast, following propagated events such as spreading depression would have required the tip of the multiprobe assembly to be concentrated in a tiny space, perceiving the same phase of the wave, unless each sensor could be located with respect to the wave front by an auxiliary signal. The second option was retained by recording the wave of the DC potential concentrically to each sensor. In addition, the complete assembly had to provide adequate protection and shielding of the high impedance ion-sensitive electrodes (K^+ and pH) and a stable enough reference junctions for use in unanesthetized animals. With K^+ surface electrodes, concentric DC potential has been proposed as the best approximation for the DC potential component to be subtracted from the sensor signal [81]. In this study we also attempted to check the accuracy of the method by recording DC potential differentially between a central barrel and the peripheral slit and to reevaluate its usefulness in correcting surface K^+ and pH measurements under various conditions.

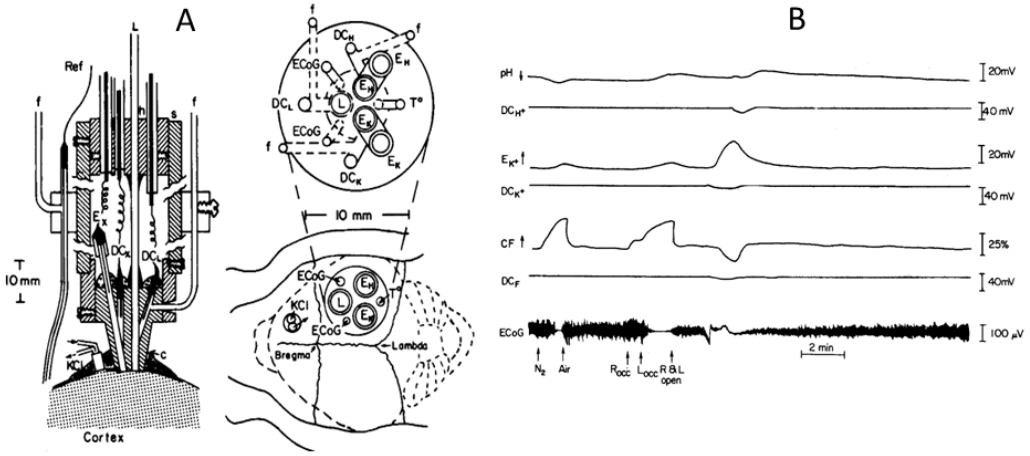

Figure 15: A. Schematic presentation of the multiprobe assembly. Left: longitudinal section of the cannula and assembly located above the cortex. A small push-pull cannula was placed near the assembly to initiate spreading depression. Right: topical view of the gerbil skull together with the location of the various electrodes with a cross section of the wide end of the cannula. B. Typical responses of the metabolic, ionic, and electrical signals, measured from an anesthetized gerbil brain, to anoxia and ischemia. Spontaneous spreading depression cycle was developed after ischemic episode [80].

Electrode Assembly:

The solution adopted for the electrode holder is basically a modification of the Lucite cannula described by Mayevsky et al. [79] for the light guide and the potassium-sensitive electrodes. To offer space for more probes, the new cannula was shaped as a truncated cone instead of a cylinder (Fig. 15A). The holes accommodating short electrode probes (K^+, pH, and pO_2) are made convergent toward the lower surface to occupy less space on the brain and divergent at the top to facilitate handling and sealing of the probes. An additional hole is drilled obliquely from the upper surface to merge with each sensor channel at about mid-distance of the lower surface. This hole accommodates an AgCl wire, used to record the local DC potential concentrically to the sensor.

The long and rigid steel stem of the light guide (L) used in this study occupies a straight vertical hole in the cannula and serves as an axis to hold the cannula (c) and the cable holder (h) at a convenient distance of each other (4 cm). Steel rods (preferentially threaded) can be used as additional or replacement pillars to fix the cannula to the cables holder. The arrangement leaves optimal access to the electrodes and electrical connections for assembling and replacement. The complete assembly is protected and shielded by a silver-pointed Lucite sleeve sliding over the cable holder. If a stronger construction is desired, the sleeve can also be permanently screwed into the cannula and cable holder, with a half-cylinder piece cut out as a removable cover. When the holder is assembled, the fixed steel pillars are screwed and/or glued in first. To protect the solder point, chloridized silver wires are glued with two-component epoxy glue in short pieces of Teflon that fit over the sensor electrode shaft and into the DC channel in the cannula. The Teflon-sleeved wires and glass tubes of the sensors are then fixed in place with hard Elephant wax and polyethylene-sleeved probes (Yellow Springs Instrument temperature probe 5U) with paraffin melted by a thermocautery tip. To avoid tension on the electrodes wires, they are connected to the input cable through a flexible coil of 36-gauge isolated copper wire (Belden).

URL: http://dx.doi.org/10.14738/bjhr.1205.19549.

Figure 15B shows a typical response of the gerbil brain to anoxia (left) and bilateral carotid occlusion (right). The initial response to anoxia is an increase of the NADH level as shown in the corrected fluorescence (CF) trace. As a result, the extracellular level of K^+ increased and returned to the base-line level after restoration of air breathing. The pH increased under anoxia, the DC potential measured in all three electrodes site (DC_{H+}, DC_{K+}, and DC_F), did not show any change during the anoxic cycle and the ECoG showed a typical depression. After occlusion of the right carotid artery (Rocc) the NADH increased by 10% compared with the normoxic level and reached only one-third of the maximal NADH level, measured during the anoxic cycle or bilateral carotid occlusion. The partial ischemia induced by Rocc did not cause any other significant changes during the short period of occlusion. After complete ischemia was induced by occlusion of the left artery (Locc, while the right one was occluded) the NADH showed a 30% increase and returned to the base-line level after both left and right arteries were reopened. During the period of complete ischemia extracellular K^+ level went up and the pH went down (more acidic). A spontaneous CSD developed during the complete ischemia, and the wave propagated to the measuring site after the two carotid arteries were reopened. During the CSD event, typical responses were recorded; namely, K^+ was elevated and then pumped back into the cells, and as a result the NADH became more oxidized (oxidation cycle). The pH showed an acidification response to the CSD. As expected the three DC potential signals showed a transient negative shift during CSD. We found that the resting level of extracellular K^+ was 3±1 mM in all undamaged brains. When the initial levels were higher, the animal was not included.

A New Model of the MPA:

The goal of this investigation was to evaluate the responses of brain tissue to CO and to attempt to elucidate differences between the physiological responses and toxic effects [82]. The affinity of CO to hemoglobin is 200 times greater than that of O_2; hence, an obvious aspect of exposure to CO is the possibility of impaired O_2 delivery and cellular hypoxia, depending on the concentration of CO. Because >50% of the energy consumed by the brain is used for the normal functions of active ion transport mechanisms, it is important to evaluate O_2 or energy balance under CO exposure. Oxygen balance can be evaluated by monitoring the level of O_2 supply compared with the O_2 demand. To monitor brain O_2 balance *in vivo* and in a continuous mode, we adopted a multiparametric monitoring approach [62,80,83] by which the hemodynamic, metabolic, ionic, and electrical activities could be examined (Fig. 16A). Our approach was to monitor the brain on the "tissue level" rather than the "cellular level." We believe that the various component elements of the brain, namely, neurons, glia cells, and capillaries, are acting as an integrated system. Therefore, we monitored the functions of the brain by using "mini probes" rather than "microprobes" that are normally used to monitor ionic homeostasis [82]. Also, the evaluation of other parameters such as cerebral blood flow (CBF) and NADH redox state were adapted to the tissue level rather than to the cellular level. Hence, our strategy was to develop a multiparametric monitoring assembly in which all the probes had the same type of contact with a small area of the brain. None of the probes penetrated the brain itself, thus avoiding severe damage to the brain or the formation of an artificial environment around the sensor that can be created around a penetrating microelectrode.

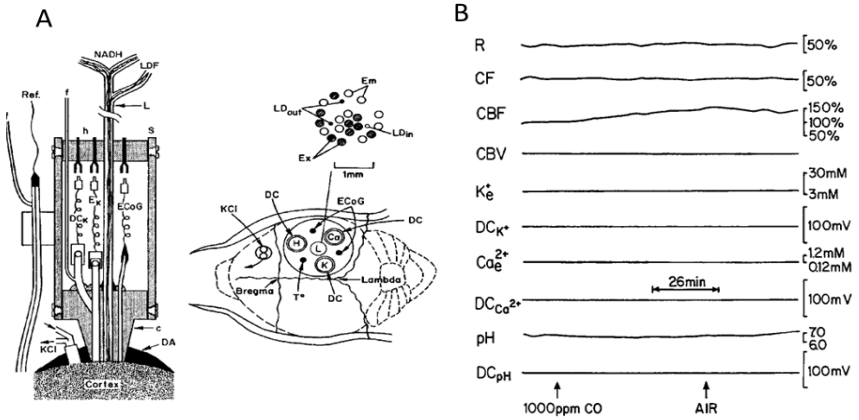

Figure 16: A. Multiprobe assembly used in awake rat to monitor hemodynamic, metabolic, ionic, and electrical activities from the brain. Left: longitudinal section. Right: location of multiprobe assembly on the skull. Ref - reference electrode; f - feeding tube of reference or other direct current electrodes; h - connectors holder; NADH - 2 arms of NADH monitoring light guide; LDF - laser Doppler flowmeter; L - light guide; s - aluminum sleeve; DCK and EK - direct current and ion specific electrodes, respectively, for K; ECoG - electrocortical electrodes; c - Plexiglas probe holder; DA - dental acrylic cement; KCl - push-pull cannula for KCl; K, Ca, and H - ion specific electrodes; DC - area of direct current steady potential monitoring; Ex and Em - excitation and emission fibers, respectively, for NADH monitoring; LDin and LDout -optical fibers for monitoring blood flow and volume, respectively; To - termistor for local temperature measurement[93]. B. Responses to 60 min of 1,000 ppm of carbon monoxide (CO) [82].

The rat was placed in an airtight Plexiglas cage. The CO at different concentrations in air (analyzed and certified by the manufacturer) was connected and flushed through the chamber. Figure 16B shows the responses of an awake rat exposed for 60 min to 1,000 ppm of CO. The main change recorded under 1,000 ppm CO was the increase in relative CBF. The CF was unchanged, suggesting no change in NADH redox state. The R and cerebral blood volume (CBV) were also very stable. The ionic homeostasis and DC potential were unaffected, as measured by the various electrodes.

The Addition of Hb Saturation to the MPA:

The basic concepts of the MPA as previously described [80,83] were adopted and modified to accommodate more probes in the same surface area of the brain [62,84]. As shown in Figure 17A, the center hole was used for the NADH light guide which was developed very recently to include fibers for relative CBF measurement by laser Doppler flowmeter [85] in addition to NADH fluorescence. In the present study two light guides were used, namely the central one (L) for NADH and CBF measurements and a microlight guide used for HbO_2 monitoring [86]. In order to prevent interference between the measurements of HbO_2 and CBF we used them alternatively with the NADH measurements. The longitudinal section of the MPA, shown on the left side of the figure, corresponds to the cross section line A shown on the right side. In order to see the two light guides in the same longitudinal section a different sectioning line would need to be used (B). Extracellular K^+ and Ca^{2+} electrodes were made by WPI Inc. (Sarasota. FL, USA) using 1.2 mm diameter PVC tubing (Cole Flex, W. Babylon. NY, USA).

The electrodes were assembled in the holder by the same basic approach described previously for the connection of the DC steady potential electrode [80]. For the DC electrode we used the

URL: http://dx.doi.org/10.14738/bjhr.1205.19549.

same electrode holder (containing Ag/AgCl pellet) provided by WPI Inc. and polyethylene tubing was connected to it and inserted into the holder. The center light guide (NADH) was covered by a rigid brass tube and was glued by a 5-minute epoxy so that after cementation to the cannula (screwed and glued) it served as an axis to hold the cannula (c) and the connector holder (h) at a fixed convenient distance.

Hemoglobin Spectrophotometry:

In order to evaluate the level of hemoglobin oxygenation we used the Erlangen microlight guide spectrophotometer EMPHO-l [84]. The light source was a water-cooled xenon high-pressure arc lamp (XBO *75*W/2Osram) operated by a starting unit and a power supply (Muller, Moosinning, Germany). The light (400-1200 nm) passing through a heat absorption filter (KGI, Schott), located between two focusing lenses, entered a central 250 μ diameter micro light guide fiber closely surrounded by a hexagon of six detecting fibers (70 μ diameter) and was transmitted to the brain surface. The emitted light from the brain was passed through a rotating interference bandpass filter disc (Anders, Nabburg) which works in the spectral domain from 502-650 run. All other details regarding data collection, calibration and calculations were published recently [86].

Since the light guide of the EMPHO was the closest probe to the KCl application site, it shows the earliest response to the CSD wave. As seen on line A, the HbO_2 trace shows an initial decrease in oxygenation followed by a larger and longer increase. The same biphasic response can be seen in the reflectance trace (R). The NADH redox slate trace (CF) shows the typical symmetrical oxidation wave, well correlated to the high activity of the Na^+K^+-ATPase keeping the ion gradient recovery after the large depolarization induced by the spreading depression. The same responses were recorded when the second and third waves passed below the MPA, as seen in lines B and C (Fig. 17B). The main difference between the three cycles developed under normoxia was the diminution of the initial decrease of the HbO_2 levels, which could also be seen when the waves were induced under hyperoxic conditions.

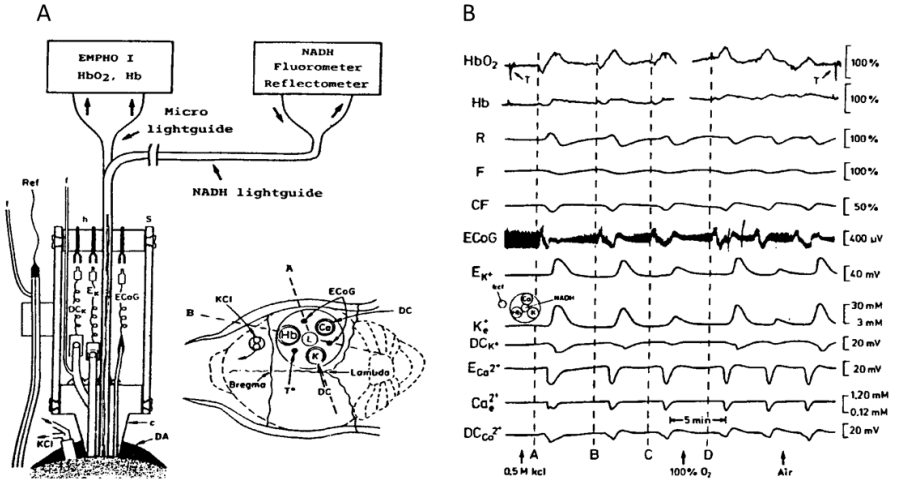

Figure 17: A. Schematic presentation of the multiprobe assembly (MPA). The longitudinal section, at the left, shows the two light guides connected to the EMPHO-I (microlight guide) and the NADH fluorometer and reflectometer (NADH light guide). At the right side of the figure the various probes are shown as located on the gerbil cerebral hemisphere. L - NADH light guide; Hb - EMPHO-light guide; K, Ca - extracellular potassium and calcium electrodes; DC - steady

potential electrodes; T - temperature probe; ECoG - electro-corticography electrodes; KCI - push-pull cannula for topical application of KCl solution; Ref - reference electrode; DCk, Ek, ECoG - cables connecting the various electrodes to the cable holder; f - filling tubes connected to the reference and the DC electrodes; C - plexiglas cannula; DA - dental acrylic cement; h, s - plexiglas cable holder and sleeve. B. The effects of cortical spreading depression on the metabolic, ionic and electrical activities of the gerbil brain. The relationship between the probes' location and the KCl (0.5 M) application site is shown inside the figure (center, left side). The gerbil was breathing air and then was switched to 100% O_2 as well as returned to air during the repeated cycles of SD [84].

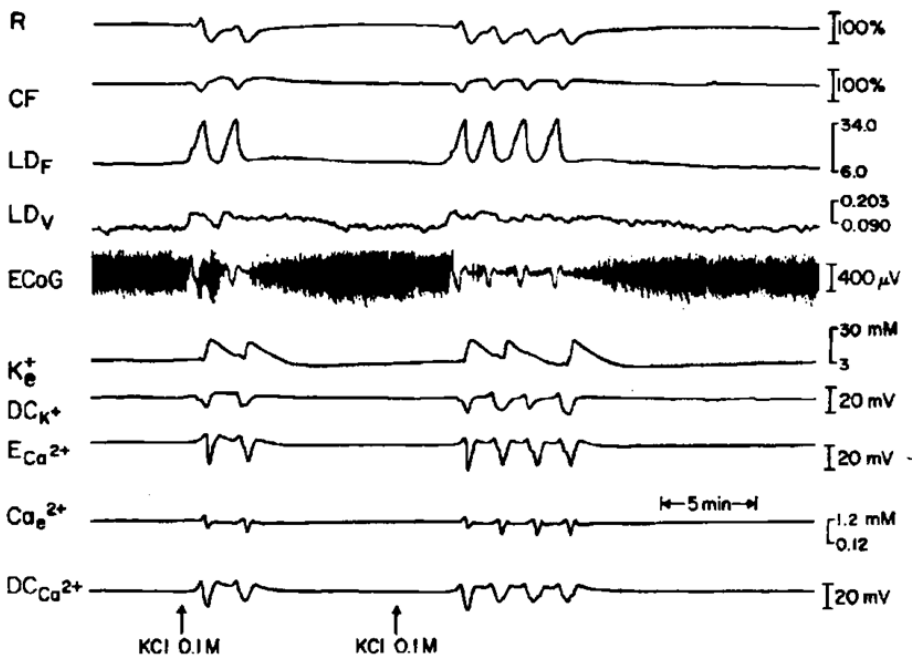

Figure 18: Metabolic hemodynamic, ionic and electrical responses to cortical spreading depression measured in rat brain. The MPA used in this study contained two different bundles of fibers for monitoring the relative CBF and NADH redox state. R, CF - reflectance and corrected fluorescence; LD_F LDv - Laser Doppler flow and volume monitored from another optic fiber located in the MPA; ECoG - electrocorticogram; K^+_e , ECa^{2+}, Ca_e^{2+} - corrected potassium, uncorrected and e a e corrected calcium ion concentrations, respectively; DC_{K+}, $DCca^{2+}$ - DC steady potential around the K^+ and Ca^{2+} electrodes [84].

MONITORING OF HUMAN BRAIN MITOCHONDRIAL NADH, MICROCIRCULATORY BLOOD FLOW AND OXYGENATION

During the last 35 years we had developed 3 types of multiparametric monitoring systems which were applied to patients at various clinical locations. The concept of our development was to provide the clinicians new physiological information that will improve the ability to diagnose the stage of pathological condition in real time. In the 1980's we developed the first multiparametric monitoring system that was adapted to experimental animals exposed to various pathological conditions [80,83,87,88]. Later on, we improved the system in order to introduce it to the neurosurgical operating room or intensive care unit (ICU) for patient monitoring. The concept behind the development was that the more parameters that are monitored, the better the diagnosis of the situation will be as presented in Figure 19A. The ideal system was to monitor eight parameters from the brain (right side) in addition to the various

URL: http://dx.doi.org/10.14738/bjhr.1205.19549.

systemic parameters monitored in every patient hospitalized (left side). The long term vision was that all parameters monitored by the 2 monitoring systems will be integrated in the same data bank and an expert system will be developed for better diagnosis of the patients. The translation of this concept into a practical tool and monitoring device is presented in Figure 19B and Figure 20.

Based on the well-developed MultiProbe Assembly (MPA) used for animal experiments [82] a new MPA was developed and applied to patients monitored in the neurosurgical operation rooms and ICU. This device allowed us to monitor, in real-time, the hemodynamic, metabolic ionic and electrical activities in the brain of comatose patients. All details regarding the technology and the clinical setup appear in our published paper [89]. Figure 19B shows the longitudinal section of the MPA (measuring 8 parameters) used in the neurosurgical operating room and ICU. The MPA was connected to the multiparametric monitoring system shown in Figure 20.

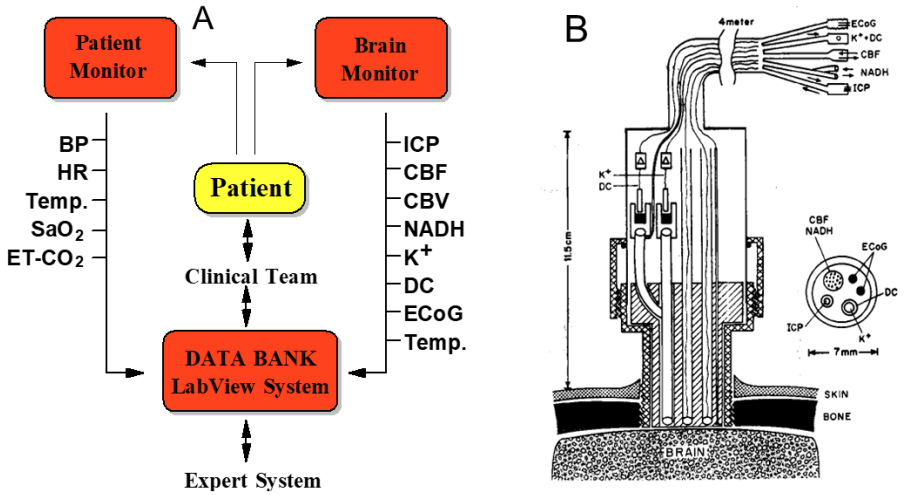

Figure 19: A. Neurological patient monitoring include usually systemic parameters (Left) however we suggest the monitoring of specific brain parameters (Right). One Data bank (LabView system) will concentrate this data which will be analyzed by the clinical team. BP-blood pressure, HR-heart rate, Temp.- body temperature, SaO_2 – oxygen saturation, ET CO_2- End Tidal CO_2, ICP-intracranial pressure, CBF, CBV- cerebral blood flow or volume, NADH-mitochondrial NADH redox state, K^+ - extracellular potassium level, DC- steady DC potential, ECoG- electrocorticography, Temp.- Brain Temperature [94]. B. Schematic representation of the multiprobe assembly (MPA) used for monitoring the brain of head-injured patients in the ICU. The MPA is connected to the brain via a special holder screwed into the skull. ICP, intracranial pressure probe; CBF, NADH-fiber optic light guide probe to measure local cerebral blood flow, (CBF) and mitochondrial redox state (NADH); K^+, DC, extracellular K^+ mini surface-electrode surrounded by a DC steady potential monitoring space; ECoG, bipolar electrocortical electrodes [89].

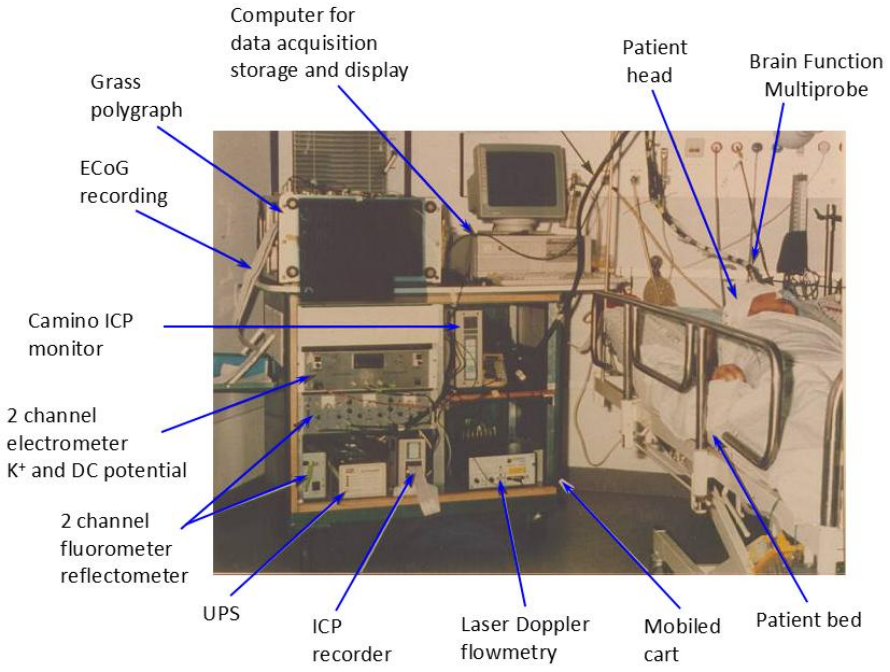

Figure 20: The first clinical monitoring setup ("Brain Monitor") used in the neurosurgical intensive care unit. - The Multiparametric monitoring system consists of various devices installed in the same cart. The MPA shown in figure 7B is connecting the brain of the patient to the Brain monitor [94].

The first attempt to monitor NADH from the human brain by our group was in 1990. We monitored few neurosurgical patients in the Hospital of the University of Pennsylvania after IRB approval. We monitored in those patients only Mitochondrial NADH and microcirculatory blood flow since extra time availability during the surgical procedure is very limited. The responses of the human brain to ischemia were presented in our publications [85]. In one patient a short brain ischemic episode was induced by the occlusion of the common carotid artery during the preparations for brain aneurysm procedure. An immediate decrease of CBF was recoded simultaneously with an increase in NADH redox state with only very small changes in the reflectance recorded (R). The recovery of CBF and NADH oxidation were very fast. The time to reach 50% of the change in NADH during the recovery was less than 3 seconds. In contrary to the NADH recovery to the pre-ischemic level, the CBF signal shows a large hyperemic response (large overshoot in CBF). The next step was to use the multiparametric monitoring system in the neurosurgical ICU. In this group, 14 patients were monitored (Fig. 21). Only one of the 14 monitored patients had developed spontaneous changes in all parameters similar to the typical responses to SD in animals. These changes were recorded 4.5h after the beginning of monitoring, which was 7 hours after admittance to the hospital. During the measuring period, this patient was bilaterally irresponsive to pain, his pupils were dilated and non- reactive to light. He was mechanically ventilated and his brain CT scan showed evidence of severe brain edema in the left hemisphere and right parietal hemorrhagic contusion. The measurements were taken from the right frontal lobe.

As seen in Figure 21A, the ECoG became depressed for 10-15 minutes and at the same time a cycle of elevated extracellular K^+ and a small negative shift in the DC potential were recorded. These changes are typical to transient depolarization, which is a dominant part of cortical

URL: http://dx.doi.org/10.14738/bjhr.1205.19549.

spreading depression (SD). NADH was oxidized while blood flow and volume increased. This patient exhibited repetitive SD cycle every 20-30 minutes. However, the following SD like cycles that were recorded from this patient (after the first ones) showed different hemodynamic and metabolic responses (Fig. 21B). While extracellular level of K^+ and the pattern of the DC potential were very similar, NADH oxidation cycles were replaced by a biphasic cycle comprised mainly of a phase of increased NADH followed by a small oxidation phase. The compensation of blood flow and volume was also reversed at this time. The monophasic increase in CBF and CBV was replaced by an initial decrease followed by a smaller increase. Significant correlations were seen between CBF, CBV and NADH (CF) and extracellular K^+ levels. Later on a spontaneous spreading depression event was developed and the response that was similar to results shown in Figure 21B.

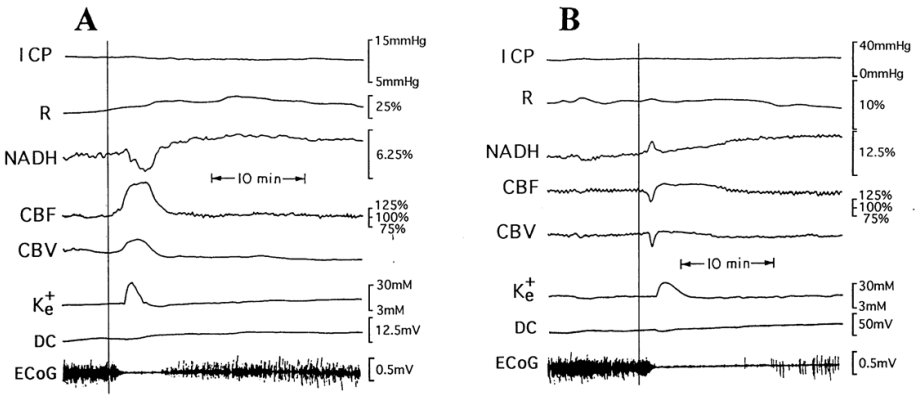

Figure 21: A - The responses of the brain to wave of cortical spreading depression developed spontaneously in a severely head injured patient. ICP - intracranial pressure; R - 366 nm reflectance, NADH - 450 nm corrected fluorescence; CBF, CBV - cerebral blood flow and volume measured by laser Doppler flowmetry; K^+_e, DC- extracellular potassium levels and the DC steady potential measured around the K^+ electrode; ECoG – electrocorticography [89]. B - Repeated response to cortical spreading depression in the same patient [95].

References

1 Chance, B. and Williams, G. R. (1955) Respiratory enzymes in oxidative phosphorylation (III- The steady state). J. Biol. Chem. 217, 409-427,

2 Chance, B. and Williams, G. R. (1955) Respiratory enzymes in oxidative phosphorylation (IV- The respiratory chain). J. Biol. Chem. 217, 429-438,

3 Chance, B., Williams, G. R., Holmes, W. F. and Higgins, J. (1955) Respiratory enzymes in oxidative phosphorylation (V- A mechanism for oxidative phosphorylation). J. Biol. Chem. 217, 439-451,

4 Chance, B. and Williams, G. R. (1955) A method for the localization of sites for oxidative phosphorylation. Nature. 176, 250-254,

5 Harden, A. and Young, W. (1906) Alcoholic ferment of yeast-juice Part II Co-ferment of yeast-juice. Proc. Roy Soc. B78, 369-375,

6 Harden, A. and Young, W. J. (1905) The influence of phosphates on the fermentation of glucose by yeast-juice: preliminary communication. Proc. Chem. Soc. (London). 21, 189-191,

7 Warburg, O., Christian, W. and Griese, A. (1935) Wasserstoff-Ubertragendes Co-ferment, seine Zusamensetzung und Wirkungsweise. Biochem. Zeitschrift. 282, 157,

8 Chance, B., Cohen, P., Jobsis, F. and Schoener, B. (1962) Intracellular oxidation-reduction states *in vivo*. Science. 137, 499-508, ^GR; NADH

9 Kohen, E., Kohen, C. and Thorell, B. (1969) Use of microfluorimetry to study the metabolism of intact cells. Biomed. Eng., 554-565, ^GR; NADH

10 Mayevsky, A. and Barbiro-Michaely, E. (2013) Shedding light on mitochondrial function by real time monitoring of NADH fluorescence: I. Basic methodology and animal studies. J. Clin. Monit. Comp. 27, 1-34,

11 Theorell, H. and Bonnichsen, R. (1951) Studies on liver alcohol dehydrogenase I. Equilibria and initial reaction velocities. Acta Chem. Scand. 5, 1105-1126,

12 Theorell, H. and Chance, B. (1951) Studies on liver alcohol dehydrogenase II. The kinetics of the compound of horse liver alcohol dehydrogenase and reduced diphosphopyridine nucleotide. Acta Chem. Scand. 5, 1127-1144,

13 Chance, B. (1951) Enzyme-substrate compounds. Adv. in Enzymology, 153-190,

14 Chance, B. and Legallias, V. (1951) Rapid and sensetive spectrophotometry. II. A stopped-flow attachment for a stabilized quartz spectrophotometer. Rev. Sci. Instr. 22, 627-638,

15 Chance, B. (1952) Spectra and reaction kinetics of respiratory pigments of homogenized and intact cells. Nature. 169, 215-221,

16 Chance, B. (1952) Respiratory pigments of metabolism cells. Federation Proc. 11,

17 Chance, B. and Neilands, J. B. (1952) Studies on lactic dehydrogenase of heart. II. A compound of lactic dehydrogenase and reduced pyridine nucleotide. J. Biol. Chem. 199, 383-387,

18 Chance, B. and Castor, L. N. (1952) Some patterns of the respiratory pigments of ascites tumors of mice. Science. 116, 200-202,

19 Chance, B. and Williams, G. R. (1954) Steady-state of reduced pyridine nucleotides in phosphorylating rat liver mitochondria. Am. Soc. Biol. Chem. 13. Abstract 633,

20 Connelly, C. M. and Chance, B. (1954) Kinetics of reduced pyridine nucleotides in stimulated frog muscle and nerve. Am. Physiol. Soc. 13, 29-,

21 Chance, B. (1954) Enzyme mechanisms in living cells. (McElroy, W. D. and Glass, B., eds.). pp. 399-453, Johns Hopkins Press, Baltimore

22 Chance, B. (1954) Spectrophotometry of intracellular respiratory pigments. Science. 120, 767-775,

23 Chance, B. and Williams, G. R. (1955) Respiratory enzymes in oxidative phosphorylation (I- Kinetics of oxygen utilization). J. Biol. Chem. 217, 383-393,

24 Chance, B. and Williams, G. R. (1955) Respiratory enzymes in oxidative phosphorylation (II- Difference spectra). J. Biol. Chem. 217, 395-407,

25 Chance, B. and Williams, G. R. (1956) The respiratory chain and oxidative phosphorylation. In Advances in Enzymology (Nord, F. F., ed.). pp. 65-134, Interscience Publisher, Inc., New York

26 Chance, B. and Connelly, C. M. (1957) A method for the estimation of the increase in concentration of adenosine diphosphate in muscle sarcosomes following a contraction. Nature. 179, 1235-1237, ^GR; NADH

27 Chance, B. (1957) Techniques for the assay of the respiratory enzymes. (Colowick, S. P. and Kaplan, N. O., eds.). pp. 273-329, Academic Press, New York

28 Chance, B. (1957) Cellular oxygen requirements. Fed. Proc. 16, 671-680, ^GR; NADH

29 Chance, B. (1959) The response of mitochondria to muscular contraction. Ann. N.Y. Acad. Sci. 81, 477-489, ^GR; NADH

30 Chance, B. and Hollunger, G. (1957) Succinate-linked pyridine nucleotide reduction in mitochondria. In Federation Proceedings, Abstract 703

31 Chance, B., Perry, R., Akerman, L. and Thorell, B. (1959) Highly sensitive recording microspectrophotometer. Rev. Sci. Instr. 30, 735-741, ^GR; NADH

URL: http://dx.doi.org/10.14738/bjhr.1205.19549.

32 Theorell, H. and Nygaard, A. P. (1954) Kinetics and equilibria in flavoprotein systems. II. The effects of pH, anions and temperature on the dissociation and reassociation of the old yellow enzyme. Acta Chem Scand. 8, 1649-1658,

33 Theorell, H. and Nygaard, A. P. (1954) Kinetics and equilibria in flavoprotein systems I. A fluorescence recorder and its application to a study of the dissociation of the old yellow enzyme and its resynthesis from riboflavin phosphate and protein. Acta Chem Scand. 8, 877-888,

34 Theorell, H., Nygaard, A. P. and Bonnichsen, R. (1954) Kinetics of alcohol dehydrogenases, studies with the aid of a fluorescence recorder. Acta Chem. Scand. 8, 1490-1491,

35 Boyer, P. D. and Theorell, H. (1956) The change in reduced diphosphopyridine nucleotide (DPNH) fluorescence upon combination with liver alcohol dehydrogenase (ADH). Acta Chem. Scand. 10, 447-450, ^GR; nadh

36 Duysens, L. N. M. and Amesz, J. (1957) Fluorescence spectrophotometry of reduced phosphopyridine nucleotide in intact cells in the near-ultraviolet and visible region. Biochim. Biophys. Acta. 24, 19-26, ^GR; NADH

37 Chance, B., Conrad, H. and Legallias, V. (1958) Simultaneous fluorimetric and spectrophotometric measurements of reaction kinetics of bound pyridine nucleotide in mitochondria. ed.)^eds.). p. 44, Paper presented at the The Biophysical Society Meeting, Cambridge, Mass. p. 44.

38 Chance, B. and Baltscheffsky, H. (1958) Respiratory enzymes in oxidative phosphorylation (VII - Binding of intramitochondrial reduced pyridine nucleotide). J. Biol. Chem. 233, 736-739, ^GR; NADH

39 Klingenberg, M., Slenczka, W. and Ritt, E. (1959) Vergleichende biochemie der pyridinnucleotid-systeme in mitochondrien verschiedener organe. Biochemische Zeitschrift. 332, 47-66, ^GR; NADH

40 Chance, B. (1959) Quantitative aspects of the control of oxygen utilization. In Ciba Foundation Symposium on Cell Metabolism ed.)^eds.). pp. 91-129, J. & A. Churchill Ltd. London, pp 91-129.

41 Chance, B. and Legallias, V. (1959) Differential microfluorimeter for the localization of reduced pyridine nucleotide in living cells. Rev. Sci. Instr. 30, 732-735, ^GR; NADH

42 Perry, R. P., Thorell, B., Akerman, L. and Chance, B. (1959) Localization and assay of respiratory enzymes in single living cells. Absorbency measurements on the Nebenkern. Nature. 184, 929-931, ^GR; NADH

43 Chance, B. and Thorell, B. (1959) Fluorescence measurements of mitochondrial pyridine nucleotide in aerobiosis and anaerobiosis. Nature. 184, 931-934, ^GR; NADH

44 Thorell, B. and Chance, B. (1959) Absorbancy measurements on liver and kidney cells. Nature. 184, 934-935, ^GR; NADH

45 Chance, B. and Jobsis, F. (1959) Changes in fluorescence in a frog sartorius muscle following a twitch. Nature. 184, 195-196, ^GR; NADH

46 Chance, B. and Thorell, B. (1959) Localization and kinetics of reduced pyridine nucleotide in living cells by microfluorometry. J. Biol. Chem. 234, 3044-3050, ^GR; NADH

47 Chance, B. and Hollunger, G. (1960) Energy-linked reduction of mitochondrial pyridine nucleotide. Nature. 185, 666-672, ^GR; NADH

48 Chance, B., Schoener, B. and Fergusson, J. J. (1962) *In vivo* induced oxidation by adrenocorticotrophic hormone of reduced pyridine nucleotide in the adrenal cortex of hypophysectomized rats. Nature. 195, 776-778, ^GR; NADH

49 Chance, B. and Schoener, B. (1962) Correlation of oxidation-reduction changes of intracellular reduced pyridine nucleotide and changes in electro-encephalogram of the rat in anoxia. Nature. 195, 956-958, ^GR; NADH

50 Chance, B., Legallias, V. and Schoener, B. (1962) Metabolically linked changes in fluorescence emission spectra of cortex of rat brain, kidney and adrenal gland. Nature. 195, 1073-1075, ^GR; NADH

51 Chance, B., Mayer, D. and Rossini, L. (1970) A time-sharing instrument for direct readout of oxidation-reduction states in intracellular compartments of cardiac tissue. IEEE Trans. Biomed. Eng. BME-17, 118-121, ^GR; NADH

52 Chance, B., Graham, N. and Mayer, D. (1971) A time sharing fluorometer for the readout of intracellular oxidation-reduction states of NADH and flavoprotein. Rev. Scientific Instr. 42, 951-957, ^GR; NADH

53 Chance, B. (1966) The identification and control of metabolic states. Genootschap ter Bevordering van Natuur-, Genees-, en Heelkunde te Amsterdam, 5-37, ^GR; NADH;6144

54 Chance, B. and Schoener, B. (1965) A correlation of absorption and fluorescence changes in ischemia of the rat liver, *in vivo*. Biochemische Zeitschrift. 341, 340-345, ^GR; NADH

55 Chance, B., Williamson, J. R., Jamieson, D. and Schoener, B. (1965) Properties and kinetics of reduced pyridine nucleotide fluorescence of the isolated and *in vivo* rat heart. Biochemische Zeitschrift. 341, 357-377, ^GR; NADH

56 Chance, B. (1967) Biochemical studies of transitions from rest to activity. The Williams & Wilkins Company, Baltimore

57 Chance, B., Schoener, B. and Schindler, F. (1963) The intracellular oxidation-reduction state. (Dickens, F. and Neil, E., eds.). pp. 367-392, Pergamon Press, London

58 Mayevsky, A. (1984) Brain NADH redox state monitored *in vivo* by fiber optic surface fluorometry. Brain Res. Rev. 7, 49-68, ^6077; 6149; 6088; 6207

59 Mayevsky, A. and Chance, B. (1982) Intracellular oxidation-reduction state measured *in situ* by a multicannel fiber-optic surface fluorometer. Science. 217, 537-540,

60 Chance, B., Oshino, N., Sugano, T. and Mayevsky, A. (1973) Basic principles of tissue oxygen determination from mitochondrial signals. Adv. Exp. Med. Biol.,. 37A, 277-292, ^GR; NADH

61 Lubbers, D. W. (1995) Optical sensors for clinical monitoring. Acta Anaesth. Scand. Suppl. 39, 37-54, ^GR; NADH

62 Mayevsky, A., et al. (1990) Oxygen supply and brain function *in vivo*: a multiparametric monitoring approach in the Mongolian gerbil. In Oxygen Transport to Tissue XII (Piper, J., Goldstick, T. K. and Meyer, M., eds.). pp. 303-313, Plenum Pub.

63 Rampil, I. J., Litt, L. and Mayevsky, A. (1992) Correlated, simultaneous, multiple-wavelength optical monitoring *in vivo* of localized cerebrocortical NADH and brain microvessel hemoglobin oxygen saturation. J. Clin. Monit. 8, 216-225,

64 Stern, M. D., et al. (1977) Continuous measurement of tissue blood flow by laser-Doppler spectroscopy. Am. J. Physiol. 232, H441-448,

65 Haberl, R. L., Heizer, M. L., Marmarou, A. and Ellis, E. F. (1989) Laser-Doppler assessment of brain microcirculation: effect of systemic alterations. Am J Physiol Heart Circ Physiol. 256, H1247-1254,

66 Dirnagl, U., Kaplan, B., Jacewicz, M. and Pulsinelli, W. (1989) Continuous measurement of cerebral cortical blood flow by laser-Doppler flowmetry in a rat stroke model. J. CBF Metab. 9, 589-596,

67 Mayevsky, A., et al. (2001) Assessment of transplanted kidney vitality by a multiparametric monitoring system. Transplant. Proc. 33, 2933-2934,

68 Mayevsky, A., et al. (1999) Optical monitoring of NADH redox state and blood flow as indicators of brain energy balance. Adv. Exp. Med. Biol. 471, 133-140,

69 Barbiro-Michaely, E., Zurovsky, Y. and Mayevsky, A. (1998) Real time monitoring of rat liver energy state during ischemia. Microvasc. Res. 56, 253-260,

70 Mayevsky, A. and Rogatsky, G. (2007) Mitochondrial function *in vivo* evaluated by NADH fluorescence: From animal models to human studies. Am. J. Physiol. Cell Physiol. 292, C615-C640,

71 Mayevsky, A., et al. (1999) Brain viability and function analyzer: multiparametric real-time monitoring in neurosurgical patients. Acta Neurochir. Suppl (Wien.). 75, 63-66,

URL: http://dx.doi.org/10.14738/bjhr.1205.19549.

72 Sonn, J. and Mayevsky, A. (2000) Effects of brain oxygenation on metabolic, hemodynamic, ionic and electrical responses to spreading depression in the rat. Brain Res. 882, 212-216,

73 Mayevsky, A., et al. (2002) The evaluation of brain CBF and mitochondrial function by a fiber optic tissue spectroscope in neurosurgical patients. Acta Neurochir. Suppl. 81, 367-371,

74 Mayevsky, A. and Chance, B. (1973) A new long-term method for the measurement of NADH fluorescence in intact rat brain with implanted cannula. Adv. Exp. Med. Biol. 37A, 239-244,

75 Mayevsky, A., Sonn, J. and Barbiro-Michaely, E. (2013) Physiological mapping of brain functions *in vivo*: Surface monitoring of hemodynamic metabolic ionic and electrical activities in real-time. J. Neurosci. Neuroeng. 2, 150-177,

76 Mayevsky, A. (1984) Brain oxygen toxicity. Invited Review. In 8th Symp. Under-water Physiol. (Bachrach, A. J. and Matzen, M. M., ed.)^eds.). pp. 69-89, Undersea Medical Society Inc, Bethesda, Maryland

77 Mayevsky, A. and Bar-Sagie, D. (1978) The interrelation between CBF, energy metabolism and ECoG in a new awake brain model. Adv. Exp. Med. Biol. 92, 761-768, ^GR; NADH

78 Mayevsky, A., Lebourdais, S. and Chance, B. (1980) The interrelation between brain PO_2 and NADH oxidation- reduction state in the gerbil. J. Neurosci. Res. 5, 173-182, ^GR; NADH; SD

79 Mayevsky, A. (1975) The effect of trimethadione on brain energy metabolism and EEG activity of the conscious rat exposed to HPO. J. Neurosci. Res. 1, 131-142, ^GR; NADH

80 Friedli, C. M., Sclarsky, D. S. and Mayevsky, A. (1982) Multiprobe monitoring of ionic, metabolic, and electrical activities in the awake brain. Am. J. Physiol. 243, R462-469,

81 Crowe, W., Mayevsky, A. and Mela, L. (1977) Application of a solid membrane ion selective electrode to *in vivo* measurements. Am. J. Physiol. 233, C56-C60,

82 Mayevsky, A., et al. (1995) Multiparametric monitoring of the awake brain exposed to carbon monoxide. J. Appl. Physiol. 78, 1188-1196, ^6088; 6207; 6097

83 Mayevsky, A. (1983) Multiparameter monitoring of the awake brain under hyperbaric oxygenation. J. Appl. Physiol. 54, 740-748,

84 Mayevsky, A., et al. (1992) Multiparametric evaluation of brain functions in the Mongolian gerbil *in vivo*. J. Basic Clin. Physiol. Pharmacol. 3, 323-342, ^6153; ysonn; 7171

85 Mayevsky, A., Flamm, E. S., Pennie, W. and Chance, B. (1991) A fiber optic based multiprobes system for intraoperative monitoring of brain functions. SPIE. 1431, 303-313,

86 Frank, K. H., Kessler, M., Appelbaum, K. and Dummler, W. (1989) The Erlangen micro-lightguide spectrophotometer EMPHO I. Phys. Med. Biol. 34, 1883-1900,

87 Mayevsky, A. and Sclarsky, D. S. (1983) Correlation of brain NADH redox state, K^+, PO_2 and electrical activity during hypoxia, ischemia and spreading depression. Adv. Exp. Med. Biol. 159, 129-141, ^GR; NADH; SD

88 Mayevsky, A., Friedli, C. M. and Reivich, M. (1985) Metabolic, ionic and electrical responses of the gerbil brain to ischemia. Am. J. Physiol. 248, R99-R107, ^6088; 7059

89 Mayevsky, A., et al. (1996) Cortical spreading depression recorded from the human brain using a multiparametric monitoring system. Brain Res. 740, 268-274,